RESEARCH ARTICLE   Open Access

Electrochemical patterns during *Drosophila* oogenesis: ion-transport mechanisms generate stage-specific gradients of pH and membrane potential in the follicle-cell epithelium

Isabel Weiß and Johannes Bohrmann[*]

Abstract

Background: Alterations of bioelectrical properties of cells and tissues are known to function as wide-ranging signals during development, regeneration and wound-healing in several species. The *Drosophila* follicle-cell epithelium provides an appropriate model system for studying the potential role of electrochemical signals, like intracellular pH (pH_i) and membrane potential (V_{mem}), during development. Therefore, we analysed stage-specific gradients of pH_i and V_{mem} as well as their dependence on specific ion-transport mechanisms.

Results: Using fluorescent indicators, we found distinct alterations of pH_i- and V_{mem}-patterns during stages 8 to 12 of oogenesis. To determine the roles of relevant ion-transport mechanisms in regulating pH_i and V_{mem} and in establishing stage-specific antero-posterior and dorso-ventral gradients, we used inhibitors of Na^+/H^+-exchangers and Na^+-channels (amiloride), V-ATPases (bafilomycin), ATP-sensitive K^+-channels (glibenclamide), voltage-dependent L-type Ca^{2+}-channels (verapamil), Cl^--channels (9-anthroic acid) and $Na^+/K^+/2Cl^-$-cotransporters (furosemide). Either pH_i or V_{mem} or both parameters were affected by each tested inhibitor. While the inhibition of Na^+/H^+-exchangers (NHE) and amiloride-sensitive Na^+-channels or of V-ATPases resulted in relative acidification, inhibiting the other ion-transport mechanisms led to relative alkalisation. The most prominent effects on pH_i were obtained by inhibiting $Na^+/K^+/2Cl^-$-cotransporters or ATP-sensitive K^+-channels. V_{mem} was most efficiently hyperpolarised by inhibiting voltage-dependent L-type Ca^{2+}-channels or ATP-sensitive K^+-channels, whereas the impact of the other ion-transport mechanisms was smaller. In case of very prominent effects of inhibitors on pH_i and/or V_{mem}, we also found strong influences on the antero-posterior and dorso-ventral pH_i- and/or V_{mem}-gradients. For example, inhibiting ATP-sensitive K^+-channels strongly enhanced both pH_i-gradients (increasing alkalisation) and reduced both V_{mem}-gradients (increasing hyperpolarisation). Similarly, inhibiting $Na^+/K^+/2Cl^-$-cotransporters strongly enhanced both pH_i-gradients and reduced the antero-posterior V_{mem}-gradient. To minor extents, both pH_i-gradients were enhanced and both V_{mem}-gradients were reduced by inhibiting voltage-dependent L-type Ca^{2+}-channels, whereas only both pH_i-gradients were reduced (increasing acidification) by inhibiting V-ATPases or NHE and Na^+-channels.

(Continued on next page)

* Correspondence: bohrmann@bio2.rwth-aachen.de
RWTH Aachen University, Institut für Biologie II, Abt. Zoologie und
Humanbiologie, Worringerweg 3, 52056 Aachen, Germany

(Continued from previous page)

Conclusions: Our data show that in the *Drosophila* follicle-cell epithelium stage-specific pH_i- and V_{mem}-gradients develop which result from the activity of several ion-transport mechanisms. These gradients are supposed to represent important bioelectrical cues during oogenesis, e.g., by serving as electrochemical prepatterns in modifying cell polarity and cytoskeletal organisation.

Keywords: *Drosophila melanogaster*, Follicle cell, Epithelium, Bioelectricity, Intracellular pH, Membrane potential, Cell polarity, Pattern formation, Ion pump, Ion channel

Background

The development and maintenance of complex multicellular structures, like tissues and organs, is controlled by an interplay of various regulatory processes. Besides genetical and biochemical mechanisms, bioelectrical phenomena, i.e. localised ion fluxes, gradients of ion concentrations, intracellular pH (pH_i) and membrane potential (V_{mem}), are known to function as wide-ranging signals to guide polarity in development, regeneration and wound-healing [1–5]. It has been shown that gradual modifications of bioelectrical properties mediate cellular processes like migration [6], proliferation [7], differentiation [8–10], and cell-cycle control [11, 12] in various species. For example, V_{mem} plays a role in specifying the left-right axis in *Xenopus* and chick embryos [13], in the regeneration of either head or tail in planarians [14], in zebrafish pigment-pattern formation [15], and in planar cell-polarity pathway regulation in *Drosophila* epithelial tissues [16]. Defects in ion transport have been associated with several human diseases, like e.g. cancer development or Alzheimer's disease, or with developmental defects caused by human channelopathies [17–21].

The generation and maintenance of electrochemical gradients within cells or tissues requires a polarised distribution and/or activation of specific ion-transport mechanisms [22, 23]. In addition, gap junctions are a prerequisite in coupling groups of cells electrically [24–26]. In contrast to classical methods, like e.g., single-cell electrode measurements, new techniques using specific fluorescent probes allow visualisation and analysis of the spatiotemporal characteristics of pH_i and V_{mem} in a large number of cells and in whole tissues [27, 28].

The follicle-cell epithelium (FCE) of the *Drosophila* ovary provides an appropriate model system for studying bioelectrical phenomena during epithelial development [29–33]. It has been shown that in *Drosophila* ovarian follicles stage-specific patterns of extracellular currents [29, 30], V_{mem} [31, 32, 34], and pH_i [32] exist that depend mainly on the exchange of protons, potassium ions and sodium ions [31, 34–36]. For studying and manipulating pH_i and V_{mem} in the FCE, we used the fluorescent pH-indicator 5-CFDA,AM and the potentiometric dye DiBAC$_4$(3) as well as several inhibitors of ion-transport mechanisms.

The *Drosophila* follicle consists of 16 germ-line cells, 15 nurse cells (NC) and one oocyte (Oo), surrounded by a single-layered somatic FCE [37]. During the course of oogenesis, the FCE differentiates into several morphologically distinct follicle-cell (FC) populations (Fig. 1a) [38–40]. In addition to establishing embryonic polarity [41] and building up the eggshell [40], the FCE plays a significant role in shaping the elongated egg [42, 43], a process which requires planar cell polarity and a polarised arrangement of the cytoskeleton.

The purpose of the present study is to clarify the roles that various ion-transport mechanisms play in regulating pH_i and V_{mem} and in generating stage-specific electrochemical gradients in the FCE. Such gradients are likely to be involved in regulating, e.g., cell polarity, cell migration, and the organisation of the cytoskeleton during oogenesis of *Drosophila*.

Results

Stage-specific pH_i-patterns

We analysed the pH_i in the FCE during the course of oogenesis. In vitellogenic stages (S8–12), we found distinct alterations of the pH_i-patterns (Figs. 1b-d and 2a; for typical follicles, see Additional file 1: Figure S1; for variability between follicles of the same stage, see Additional file 2: Table S1).

Antero-posterior gradient

In S8, the pH_i in the FCE is relatively acidic compared to the pH_i in the germ-line cells. An antero-posterior (a-p) gradient is visible, with more alkaline pH_i in the anterior FC (aFC) and more acidic pH_i in the posterior FC (pFC). In S9 and 10a, the a-p gradient reverses and the centripetal FC (cFC) show more acidic pH_i than the pFC. At S10b, this a-p gradient becomes very distinct and is preserved during S11 and 12. In contrast to earlier stages, the pH_i in the FCE is now more alkaline compared to the pH_i in the germ-line cells.

Dorso-ventral gradient

In S8, the FCE does not yet exhibit a dorso-ventral (d-v) gradient. A significant gradient with relatively acidic dorsal and relatively alkaline ventral FC arises in S9 and increases during S10b-12.
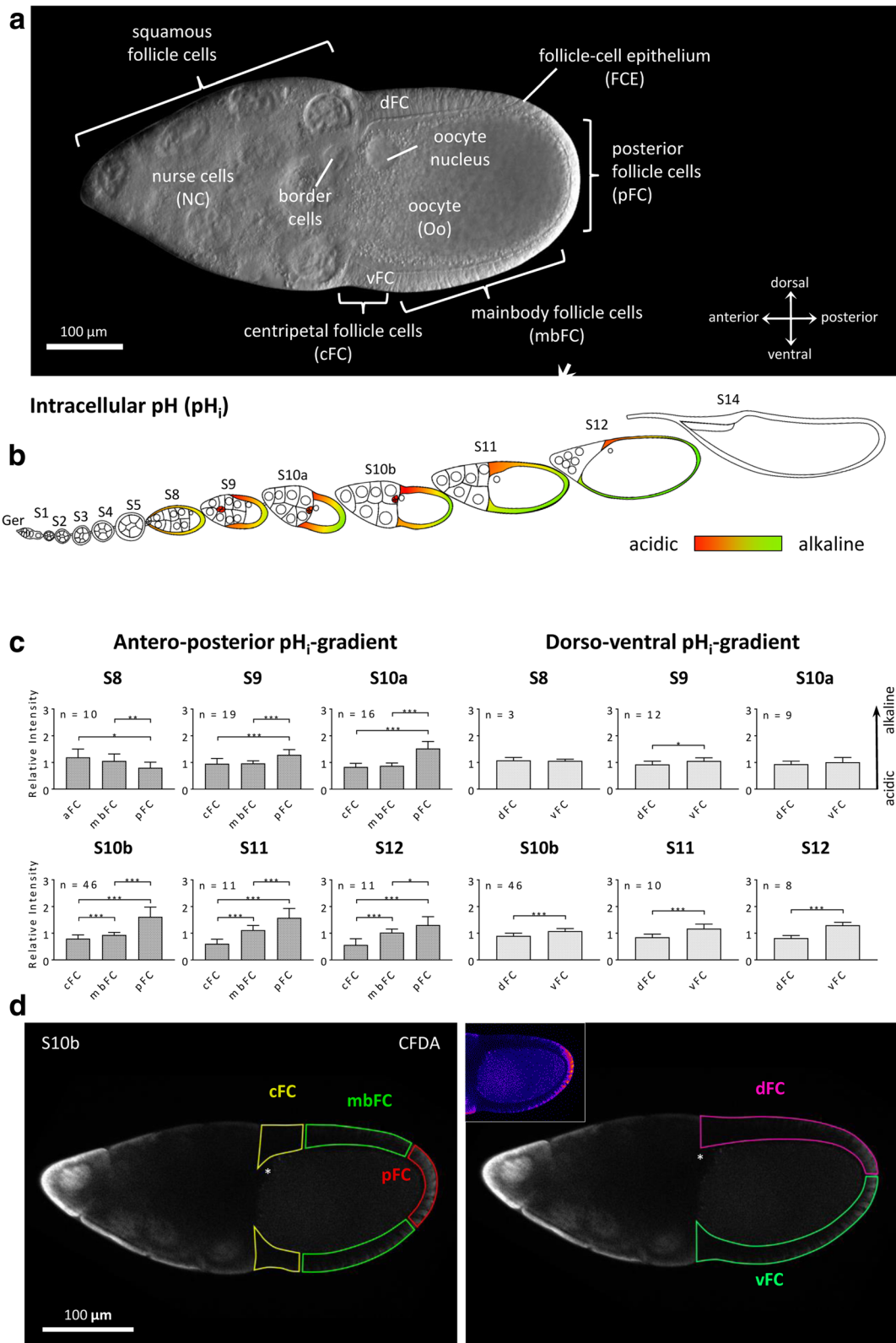
Fig. 1 (See legend on next page.)

(See figure on previous page.)

Fig. 1 Development of pH_i-gradients in the FCE during S8–12 (CFDA; SIM). **a** Types of germ-line and somatic cells of the *Drosophila* follicle. At stage 10b (S10b), the oocyte (Oo, posterior) constitutes almost one half of the follicle's volume. The anterior half is formed by 15 nurse cells (NC). The 16 germ-line cells (Oo and NC) are covered by a single-layered somatic follicle-cell epithelium (FCE). The columnar FCE surrounding the oocyte is subdivided into three follicle-cell (FC) populations: centripetally migrating FC (cFC), mainbody FC (mbFC) and posterior FC (pFC). The dorsal FCE (dFC) is thicker than the ventral FCE (vFC). Squamous FC surround the NC population. The oocyte nucleus and the border cells, a cluster of migratory follicle cells, lie close to each other near the dorsal side (DIC image). **b** Schematic drawing of an ovariole showing pH_i in the analysed stages S8–12 (cf. Additional file 1: Figure S1 for examples; Ger, germarium). **c** In S8, anterior FC (aFC) are more alkaline compared to pFC. During S9–12, an antero-posterior (a-p) gradient establishes with relatively acidic cFC and relatively alkaline pFC. From S9 and, in particular, from S10b onwards, a dorso-ventral (d-v) gradient with relatively alkaline vFC and relatively acidic dFC develops. To analyse the a-p and d-v gradients, the fluorescence intensities of the different FC types ($3 \leq n \leq 46$ follicles per stage) were measured and normalised using the fluorescence intensity in the whole FCE of the respective follicle (*relative intensity*). Mean values, shown with their standard deviation (cf. Additional file 2: Table S1), were compared using an unpaired t-test (* $p < 0.05$; ** $p < 0.01$; *** $p < 0.001$). **d** Optical median sections of a CFDA-stained S10b-follicle. Inset shows a pseudocolour image of the same section. Low fluorescence intensity (blue) indicates lower pH_i (relatively acidic) while high fluorescence intensity (pink) indicates higher pH_i (relatively alkaline). Asterisk, oocyte nucleus (dorsal)

Stage-specific V_{mem}-patterns

During the course of vitellogenesis (S8–12), we also observed distinct changes in the V_{mem}-patterns (Fig. 2; for typical follicles, see Additional file 1: Figure S2; for variability between follicles of the same stage, see Additional file 2: Table S2).

Antero-posterior gradient

Up to S8, all FC show a similar V_{mem} which is relatively depolarised compared to the germ-line cells. At S9 and 10a, an a-p gradient starts to establish with relatively depolarised FC in the centripetal and posterior regions of the follicle (cFC and pFC) compared to the mainbody FC (mbFC). During S10b-12, the gradient changes so that only the pFC are depolarised compared to mbFC and cFC.

Dorso-ventral gradient

During S8-10a, a significant d-v gradient could not be detected in the FCE. However, a d-v gradient emerges during S10b-12, with relative depolarisation on the ventral side of the follicle (vFC). Dorsal cFC show a striking increase in depolarisation during late S10b and 11. But on average, the dorsal FCE is hyperpolarised compared to the ventral FCE.

Inhibition of ion-transport mechanisms

Six inhibitors were used to determine the roles that specific ion-transport mechanisms play in the regulation of pH_i and V_{mem} as well as in the generation of electrochemical gradients in the FCE during S10b. We found that either pH_i or V_{mem} or both parameters were affected by each tested inhibitor.

Effects of inhibitors on pH_i
WFM-experiment

The inhibitors furosemide ($Na^+/K^+/2Cl^-$-cotransporters), glibenclamide (ATP-sensitive K^+-channels), 9-anthroic acid (Cl^--channels) and verapamil (L-type Ca^{2+}-channels) showed significant alkalising effects in the FCE. The inhibitors amiloride (NHEs and Na^+-channels) and bafilomycin (V-ATPases) had no significant effects on the pH_i in the FCE under these experimental conditions. The strongest effects were observed with both glibenclamide and furosemide (Fig. 3, Additional file 2: Table S3).

SIM-experiment

The treatment with the inhibitors furosemide, glibenclamide, 9-anthroic acid and verapamil, respectively, resulted again in alkalisation. These effects were significant in all types of FC and particularly distinct with furosemide and glibenclamide (Figs. 4 and 5a, Additional file 2: Table S5). Amiloride led to slight acidification which was significant in pFC. The increase in fluorescence intensity elicited by bafilomycin was due to granular staining in the FCE (Fig. 5 b). Considering the localisation of V-ATPases in plasma membranes and in vesicle membranes of FC [33, 46], it is obvious that bafilomycin caused alkalisation of vesicles, while the cytoplasm of FC became more acidic. Modifications of the a-p and/or d-v pH_i-gradients were observed with all tested inhibitors. The influences were particularly strong with both glibenclamide and furosemide, which enhanced the a-p and d-v gradients (increasing angle; alkalisation), as did verapamil. 9-Anthroic acid resulted in a shallower d-v gradient (decreasing angle; acidification) because of its stronger effect on vFC, whereas the a-p gradient became slightly enhanced (alkalisation). Amiloride, on the other hand, led to both shallower a-p and d-v gradients (acidification), as did bafilomycin (increasing cytoplasmic acidification due to increasing vesicle alkalisation). The inclinations of the gradients were inferred from the mean values of relative fluorescence intensity depicted in Figs. 4b and 5a.

Effects of inhibitors on V_{mem}
WFM-experiment

Almost all tested inhibitors (verapamil, amiloride, 9-anthroic acid, furosemide and bafilomycin) had significant hyperpolarising effects on the V_{mem} in the FCE. The strongest effect was observed with verapamil, the weakest with bafilomycin. Glibenclamide caused a slight

Fig. 2 (See legend on next page.)
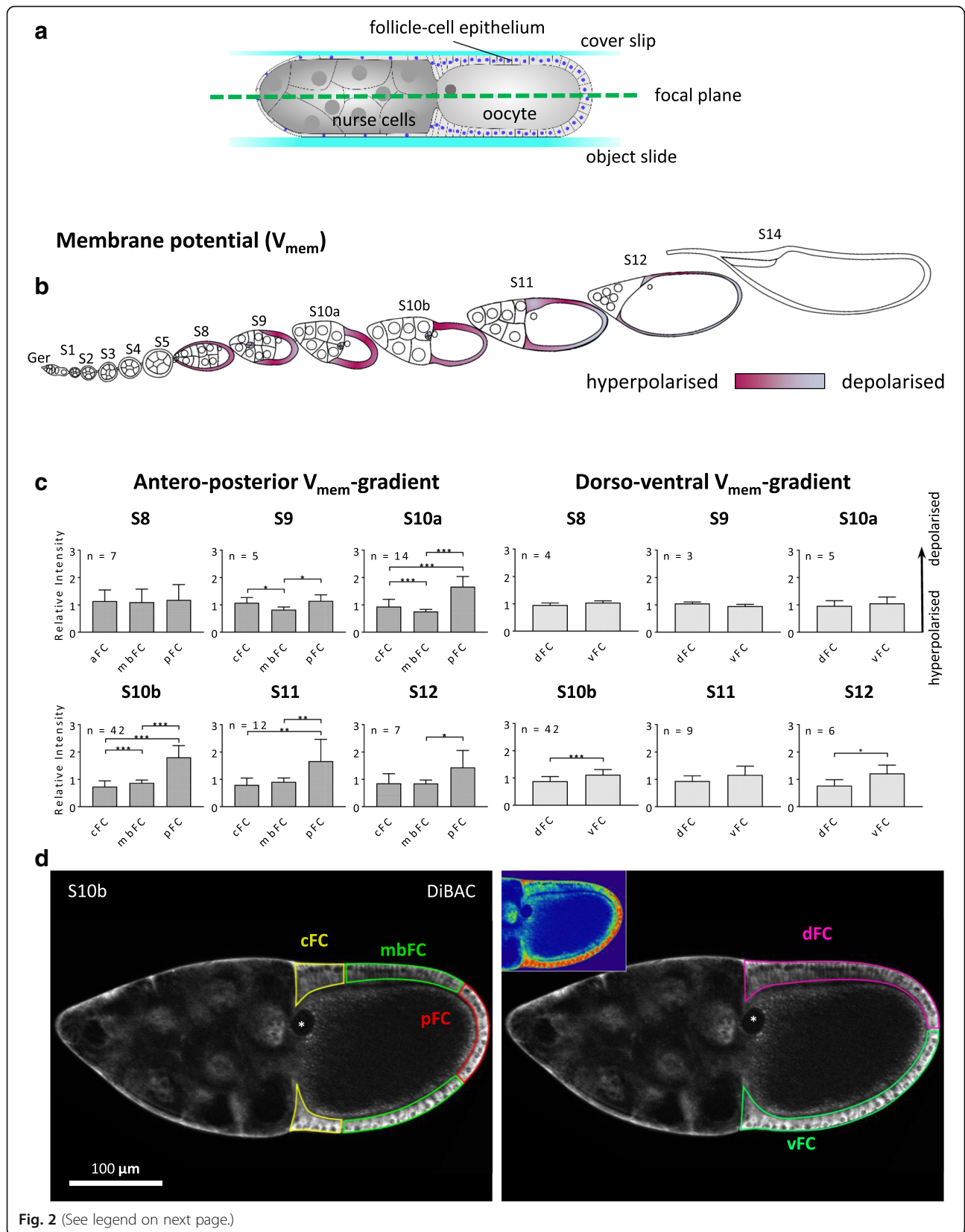
(See figure on previous page.)

Fig. 2 Development of V_{mem}-gradients in the FCE during S8–12 (DiBAC; SIM). **a** Schematic drawing of a S10b-follicle placed between an object slide and a cover slip. The focal plane of median optical sections generated by the ApoTome (SIM) is shown as dashed green line. **b** Schematic drawing of an ovariole showing V_{mem} in the analysed stages S8–12 (cf. Additional file 1: Figure S2 for examples). **c** During S9–12, an a-p gradient establishes with relatively hyperpolarised cFC and relatively depolarised pFC. From S10b onwards, a d-v gradient with relatively depolarised vFC and relatively hyperpolarised dFC develops (cf. Additional file 2: Table S2). For abbreviations and statistics, see legend to Fig. 1. **d** Optical median sections of a DiBAC-stained S10b-follicle. Inset shows a pseudocolour image of the same section. Low fluorescence intensity (green) indicates relative hyperpolarisation while high fluorescence intensity (red) indicates relative depolarisation

hyperpolarisation which was not significant. Depolarisation was not observed (Fig. 6, Additional file 2: Table S4).
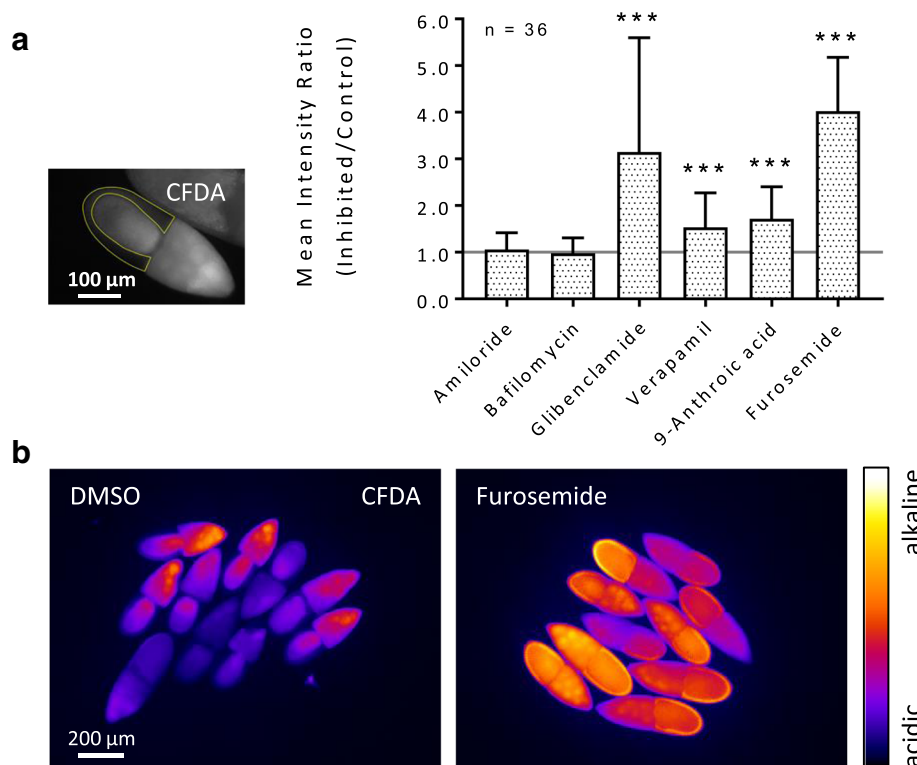
SIM-experiment

All inhibitors caused more or less hyperpolarisation in the FCE (Figs. 7 and 8, Additional file 2: Table S6). The strongest effects on V_{mem} were observed with verapamil and glibenclamide, the weakest with amiloride and bafilomycin (not significant). Glibenclamide and verapamil lowered the a-p gradient as well as the d-v gradient (decreasing angle; hyperpolarisation), whereas furosemide and 9-anthroic acid had prominent decreasing effects only on the a-p gradient. The inclinations of the gradients were inferred from the mean values of relative fluorescence intensity depicted in Figs. 7b and 8.

Discussion

Stage-specific pH_i- and V_{mem}-gradients are established in the FCE

We have shown that the FCE exhibits stage-specific a-p and d-v gradients of pH_i and V_{mem}, respectively, which

Fig. 3 Inhibitors of ion-transport mechanisms exert influence on the pH_i in the FCE during S10b (WFM-experiment; CFDA). **a** WFM-fluorescence images were used to measure the fluorescence intensity in the columnar FCE (marked yellow) of every single follicle. While glibenclamide (ATP-sensitive K^+-channels) and furosemide ($Na^+/K^+/2Cl^-$-cotransporters) led to strong alkalisation, the alkalising effects of verapamil (L-type Ca^{2+}-channels) and 9-anthroic acid (Cl^--channels) were smaller. Amiloride (NHEs and Na^+-channels) and bafilomycin (V-ATPases) showed no significant effects. To analyse and compare the effects of the inhibitors, averaged values (of 12 time points during 60 min of inhibition) of three experiments per inhibitor were summed up and normalised (*mean intensity ratio*). Mean values, shown with their standard deviation (cf. Additional file 2: Table S3), were compared using an unpaired t-test (* $p < 0.05$; ** $p < 0.01$; *** $p < 0.001$). **b** Pseudocolour fluorescence images after 60 min of incubation. Furosemide led to strong alkalisation of the whole follicle. In contrast to the control (DMSO), the columnar FCE exhibits an even stronger fluorescence intensity than the germ-line cells

Fig. 4 (See legend on next page.)
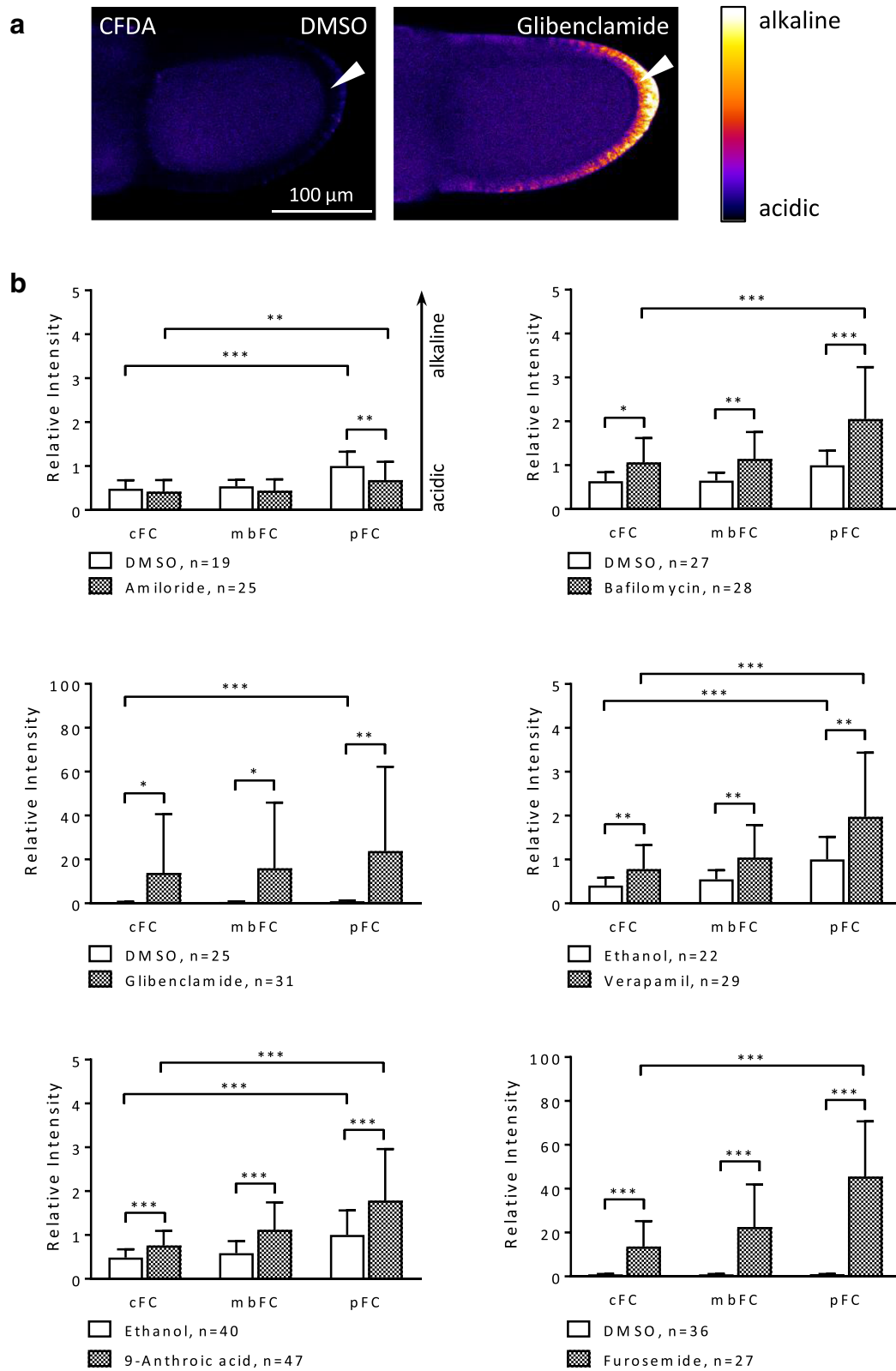
(See figure on previous page.)

Fig. 4 The a-p pH_i-gradient in the FCE is affected by all inhibitors during S10b (SIM-experiment; CFDA). **a** Pseudocolour SIM-fluorescence images of S10b-follicles. Compared to the control (DMSO), blocking with glibenclamide for 20 min resulted in strong alkalisation of the FCE which was most prominent in pFC (arrowhead). **b** Especially glibenclamide and furosemide, but also verapamil and 9-anthroic acid led to alkalisation in all FC types. Glibenclamide and furosemide resulted in a considerably steeper a-p gradient (enlargement of the angle × 20 and × 150, respectively). Verapamil and 9-anthroic acid enhanced the a-p gradient as well, but to a lesser extent (both × 2). The increase in fluorescence intensity as well as in the inclination of the a-p gradient (× 2) caused by bafilomycin was due to the alkalisation of vesicles (see Fig. 5 b) and, therefore, to the acidification of the cytoplasm resulting in a shallower a-p gradient. Amiloride led to acidification of pFC, thus slightly reducing the angle of the a-p gradient (× 0.5) as well. For each inhibitor, at least five repetitions of the experiment were performed. Normalised values of the single experiments were merged into one evaluation (*relative intensity*). Mean values, shown with their standard deviation (cf. Additional file 2: Table S5), were compared using an unpaired t-test (* $p < 0.05$; ** $p < 0.01$; *** $p < 0.001$)

are most distinctive during S10b. The pH_i- and V_{mem}-gradients arise approximately at the same stage, but they are not congruent. The pH_i increases (alkalisation) from anterior (cFC) to posterior (pFC) and from dorsal (dFC) to ventral (vFC), and, therefore, the dorsal cFC possess the most acidic pH_i.

In a-p direction, the developing V_{mem}-gradient differs from the pH_i-gradient. Since the mbFC are relatively hyperpolarised compared to the cFC and pFC, no continuous a-p V_{mem}-gradient exists. However, from dFC to vFC, the V_{mem} becomes continuously depolarised. For both pH_i and V_{mem}, the stages differ during which the a-p and d-v gradients become established. Since they start in S9, the a-p gradients are already existing when the d-v gradients become obvious during S10b.

It is expected that the establishment of electrochemical gradients is depending on the asymmetric distribution and/or activity of ion-transport mechanisms in different types of FC. Recent studies have shown that e.g. gap junctions, V-ATPases, Na^+/K^+-pumps and Na^+-channels are enriched in certain regions of the FCE compared to other regions [32, 33, 36, 44–46]. To function as temporal and spatial signals during development, electrochemical gradients and/or local changes of pH_i and V_{mem} have to be translated into cellular responses. For example, this could be achieved by voltage-dependent L-type Ca^{2+}-channels that become asymmetrically activated in the FCE [32].

Inhibitors of ion-transport mechanisms affect pH_i and V_{mem} in the FCE

To identify mechanism that are involved in regulating pH_i and V_{mem} in the FCE, we used inhibitors of several ion-transport mechanisms that have already been detected and/or localised in the *Drosophila* ovary [32, 33, 44, 47–50]. All used inhibitors affected either pH_i or V_{mem} or both parameters in S10b (for summary, see Fig. 9). If an inhibitory effect was detectable, it could be observed throughout the entire columnar FCE - though, in different FC types, often to varying extents.

The most prominent effects on pH_i were obtained with both glibenclamide (ATP-sensitive K^+-channels) and furosemide ($Na^+/K^+/2Cl^-$-cotransporters). These

inhibitors led to strong relative alkalisation in all FC types by blocking H^+-transport indirectly. Inhibition of ATP-sensitive K^+-channels by glibenclamide reduces K^+-efflux. Since the intracellular K^+-concentration and the pH_i are known to be interrelated, a higher intracellular K^+-concentration would reduce H^+-influx (K^+/H^+-antiport [51, 52]). In addition, it has been shown that K^+-uptake into *Drosophila* follicles is strongly dependent on extracellular pH [36]. $Na^+/K^+/2Cl^-$-cotransport, which can be blocked by furosemide (or bumetanide, an analogue of furosemide), is typically coupled with Cl^-/HCO_3^--antiport, so that furosemide has no impact on Cl^--transport in total [53, 54]. Due to this coupling, HCO_3^--transport might be affected, causing a change of pH_i in the FCE [55, 56]. The alkalisation obtained with 9-anthroic acid, which blocks Cl^--channels, is also likely to be due to an effect on Cl^-/HCO_3^--antiport.

Amiloride (NHEs and Na^+-channels) and bafilomycin (V-ATPases), that are both direct inhibitors of H^+-transport, led to slight acidification of the FCE. While NHEs are known for their role in pH_i-homeostasis [47, 56–58], one of the key functions of V-ATPases, besides acidification of cytoplasmic vesicles, is to energise the plasma membranes of most insect cells [59, 60]. Since the generated H^+-gradient drives secondary active transport mechanisms like NHEs [51, 60], a strong effect of bafilomycin on pH_i was not expected. Similarly, the relatively small impact of amiloride on pH_i is supposed to be due to compensatory effects exerted by other ion transporters.

V_{mem} in the FCE was clearly influenced by glibenclamide (ATP-sensitive K^+-channels) and, most strongly, by verapamil (voltage-dependent L-type Ca^{2+}-channels). Although Ca^{2+}-channels are not likely to contribute much to V_{mem} directly, blocking of Ca^{2+}-influx can result in diverse cellular reactions, since Ca^{2+} is a second messenger [61]. A strong effect of amiloride on V_{mem} was not expected, since Na^+/H^+-antiport is electroneutral. Moreover, the effect of blocking Na^+-channels is relatively weak and can be compensated by other ion-transport mechanisms. Compensatory effects always have to be taken into account, and they are supposed to be the reason for the absence of a strong impact of bafilomycin
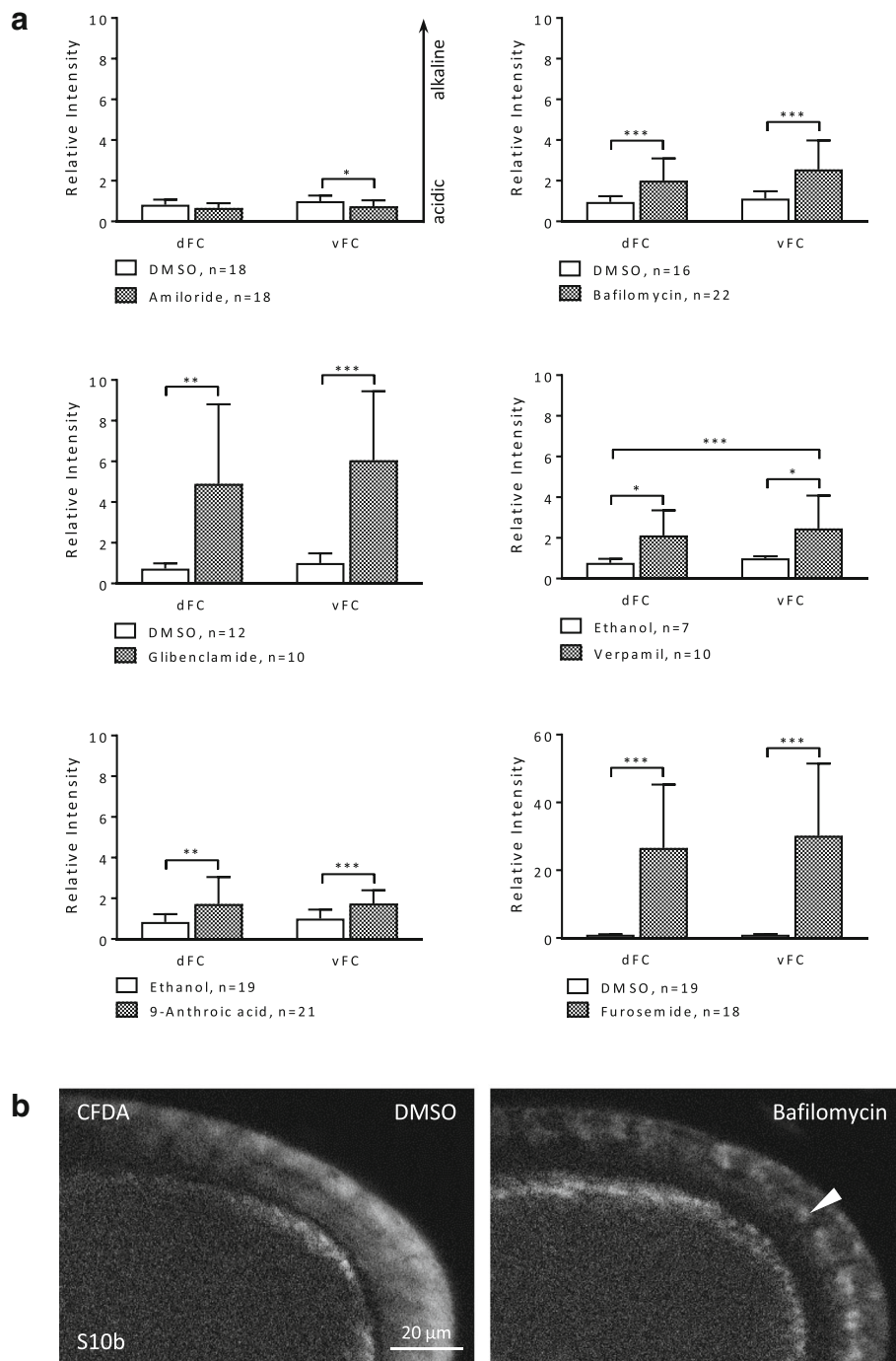
Fig. 5 a All inhibitors exert influence on the d-v pH$_i$-gradient in the FCE during S10b (SIM-experiment; CFDA). Especially glibenclamide and furosemide, but also verapamil and 9-anthroic acid led to alkalisation in both FC types. Verapamil, glibenclamide, and furosemide resulted in a steeper d-v gradient (angle × 2, × 5, and × 100, respectively). The increase in fluorescence intensity as well as in the inclination of the d-v gradient (× 3) caused by bafilomycin was due to the alkalisation of vesicles (see **b**), leading to increasing cytoplasmic acidification as well as to a shallower d-v gradient. Amiloride and 9-anthroic acid led to a stronger acidification of vFC, thus reducing the angle of the d-v gradient (× 0.5 and × 0.1, respectively) as well (cf. Additional file 2: Table S5). For statistics, see legend to Fig. 4. **b** Alkalisation of vesicles in the FCE by bafilomycin. SIM-fluorescence images of S10b-follicles incubated in R-14 medium with bafilomycin or with DMSO (control) for 20 min. Inhibition of V-ATPases led to a more granular staining (arrowhead) compared to the controls, indicating alkalisation of vesicles. In addition, the cytoplasm of the FC appeared darker than in the controls, indicating cytoplasmic acidification
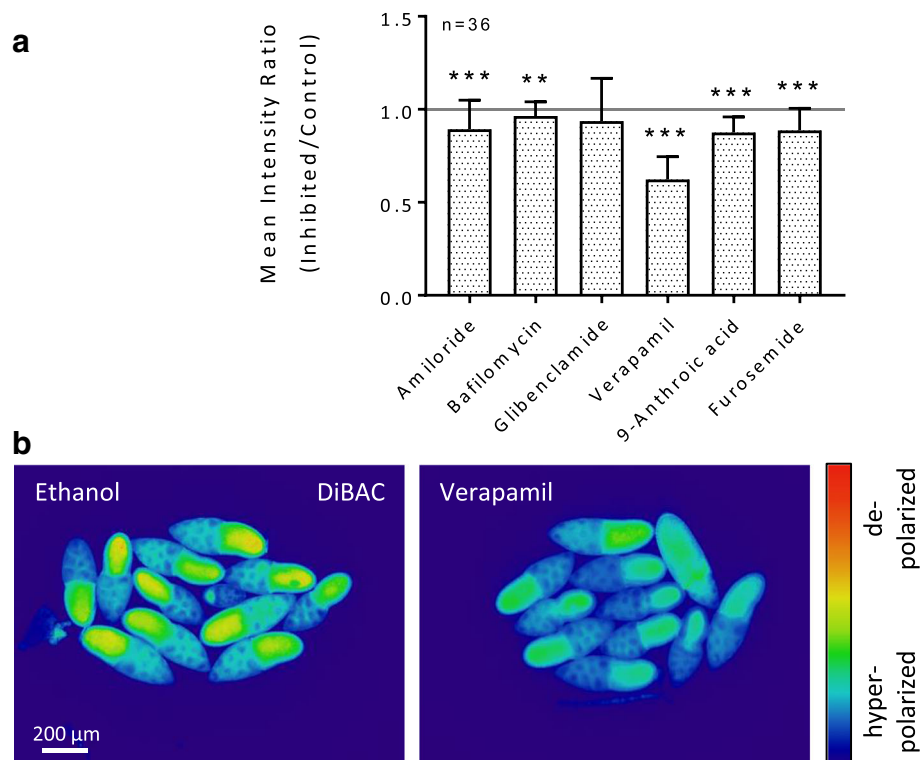
Fig. 6 Inhibitors of ion-transport mechanisms exert influence on the V_{mem} in the FCE during S10b (WFM-experiment; DiBAC). **a** WFM-fluorescence images were used to measure the fluorescence intensity in the columnar FCE of every single follicle. The measured area was as shown in Fig. 3 a. While verapamil led to strong hyperpolarisation, amiloride, bafilomycin, 9-anthroic acid, and furosemide led to slight hyperpolarisation. The hyperpolarising effect of glibenclamide was not significant (cf. Additional file 2: Table S4). For abbreviations and statistics, see legend to Fig. 3. **b** Pseudocolour fluorescence images after 60 min of incubation. Verapamil led to a strong decrease in fluorescence intensity (hyperpolarisation) in the whole follicle

(V-ATPases) on V_{mem} as well. Similarly, inhibition with furosemide ($Na^+/K^+/2Cl^-$-cotransporters) and 9-anthroic (Cl^--channels) had only minor effects on V_{mem}.

Inhibitors of ion-transport mechanisms affect pH_i- and V_{mem}-gradients in the FCE

Since with some inhibitors different types of FC were affected to different extents, the a-p and/or d-v gradients during S10b became modified in several ways (for summary, see Fig. 10).

The treatment with glibenclamide (ATP-sensitive K^+-channels) resulted in both an enhancement of the a-p and d-v pH_i-gradients (increasing alkalisation) and a reduction of the a-p and d-v V_{mem}-gradients (increasing hyperpolarisation). This could be due to the higher concentrations of ATP-sensitive K^+-channels found in dorsal cFC (unpublished results). It has been shown that both acidic pH and low K^+-concentrations result in reduced gap-junctional communication in *Drosophila* follicles [48]. Therefore, glibenclamide is supposed to enhance gap-junctional communication via higher intracellular K^+-concentrations as well as alkalisation of pH_i, leading to increasing hyperpolarisation in the V_{mem}-gradients. Furosemide ($Na^+/K^+/2Cl^-$-cotransporters) also led to

markedly steeper a-p and d-v pH_i-gradients as well as to a shallower a-p V_{mem}-gradient. Whether these effects depend on an unequal distribution of $Na^+/K^+/2Cl^-$-cotransporters remains to be analysed. Likewise, the distributions of NHEs (amiloride) as well as Cl^--channels (9-anthroic acid), which both modified electrochemical gradients in the FCE, are not yet known. However, it has been shown that V-ATPases are accumulated in the membranes of pFC and vFC [32, 33]. A stronger effect of bafilomycin on these FC types led to reduction of a-p and d-v pH_i-gradients (increasing cytoplasmic acidification due to increasing vesicle alkalisation). The application of verapamil both enhanced the a-p and d-v pH_i-gradients and reduced the a-p and d-v V_{mem}-gradients (increasing hyperpolarisation). This is in accordance with the observed higher concentrations of activated L-type Ca^{2+}-channels in pFC and vFC [32]. It is known that high intracellular Ca^{2+}-concentrations result in reduced gap-junctional communication in *Drosophila* follicles [46]. Therefore, verapamil is supposed to enhance gap-junctional communication by lowering intracellular Ca^{2+}-concentrations, leading to both increasing alkalisation in pH_i-gradients and increasing hyperpolarisation in V_{mem}-gradients.
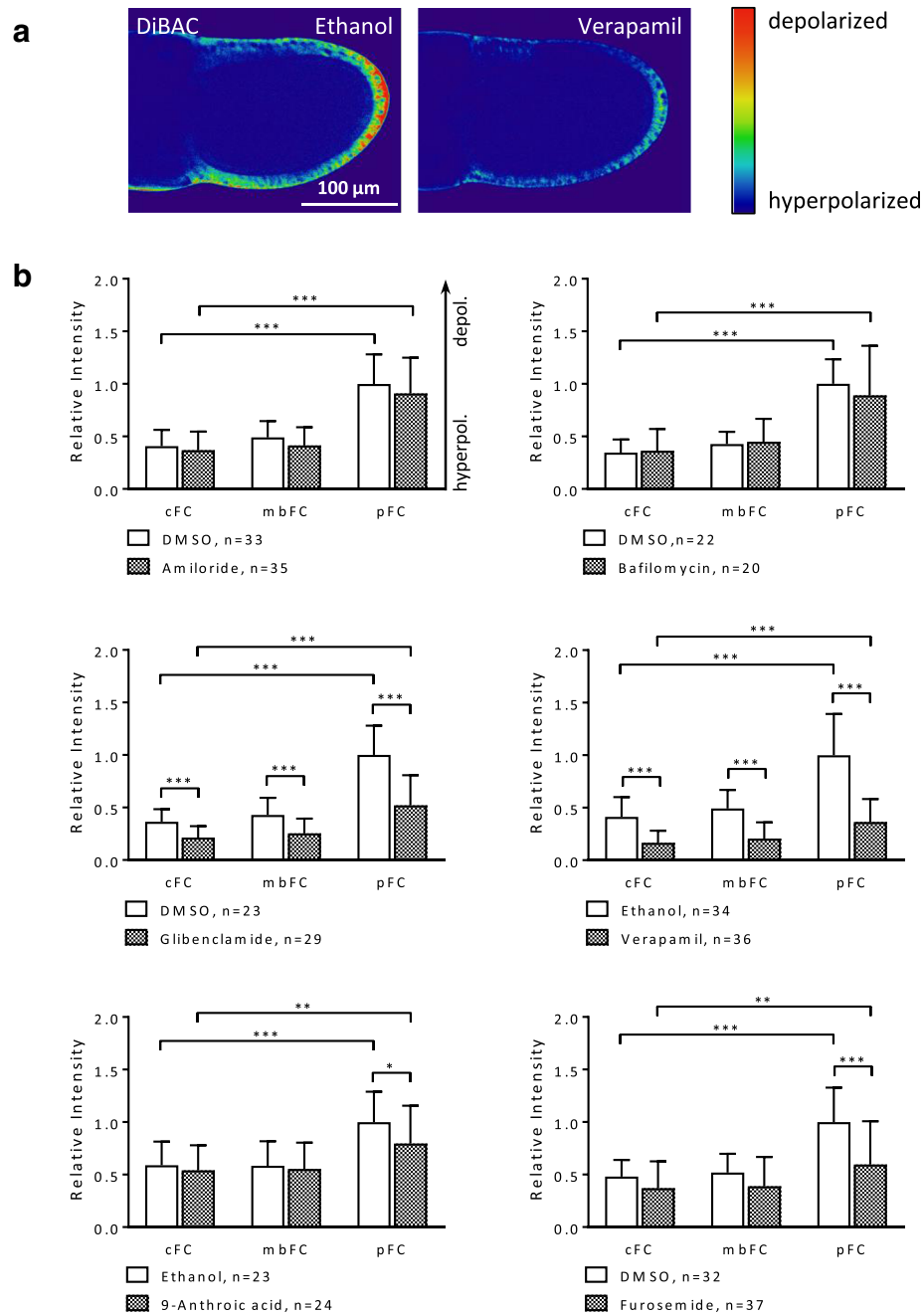
Fig. 7 The a-p V_{mem}-gradient in the FCE is affected by most inhibitors during S10b (SIM-experiment; DiBAC). **a** Pseudocolour SIM-fluorescence images of S10b-follicles. Compared to the control (ethanol), blocking with verapamil for 20 min resulted in strong hyperpolarisation of the FCE. **b** Glibenclamide and verapamil led to strong hyperpolarisation in all FC types, but especially in pFC, thus lowering the inclination of the a-p gradient (angle × 0.5 and × 0.3, respectively). Furosemide and 9-anthroic acid hyperpolarised only the pFC, thereby lowering the a-p gradient as well (both × 0.5). Amiloride and bafilomycin showed no significant effects on the a-p gradient (cf. Additional file 2: Table S6). For statistics, see legend to Fig. 4

Conclusion

In the FCE of *Drosophila*, gap junctions and ion-transport mechanisms, like NHEs, Na^+-channels, V-ATPases, ATP-sensitive K^+-channels, voltage-dependent L-type Ca^{2+}-channels, Cl^--channels and $Na^+/K^+/2Cl^-$-cotransporters, are involved in the generation of stage-specific pH_i- and V_{mem}-gradients. Since bioelectrical phenomena are known to affect, e.g., cytoskeletal dynamics, such gradients are supposed to serve as electro-chemical prepatterns that control planar cell polarity and guide gradual changes in cytoskeletal organisation. In the FCE, a particular arrangement of cytoskeletal
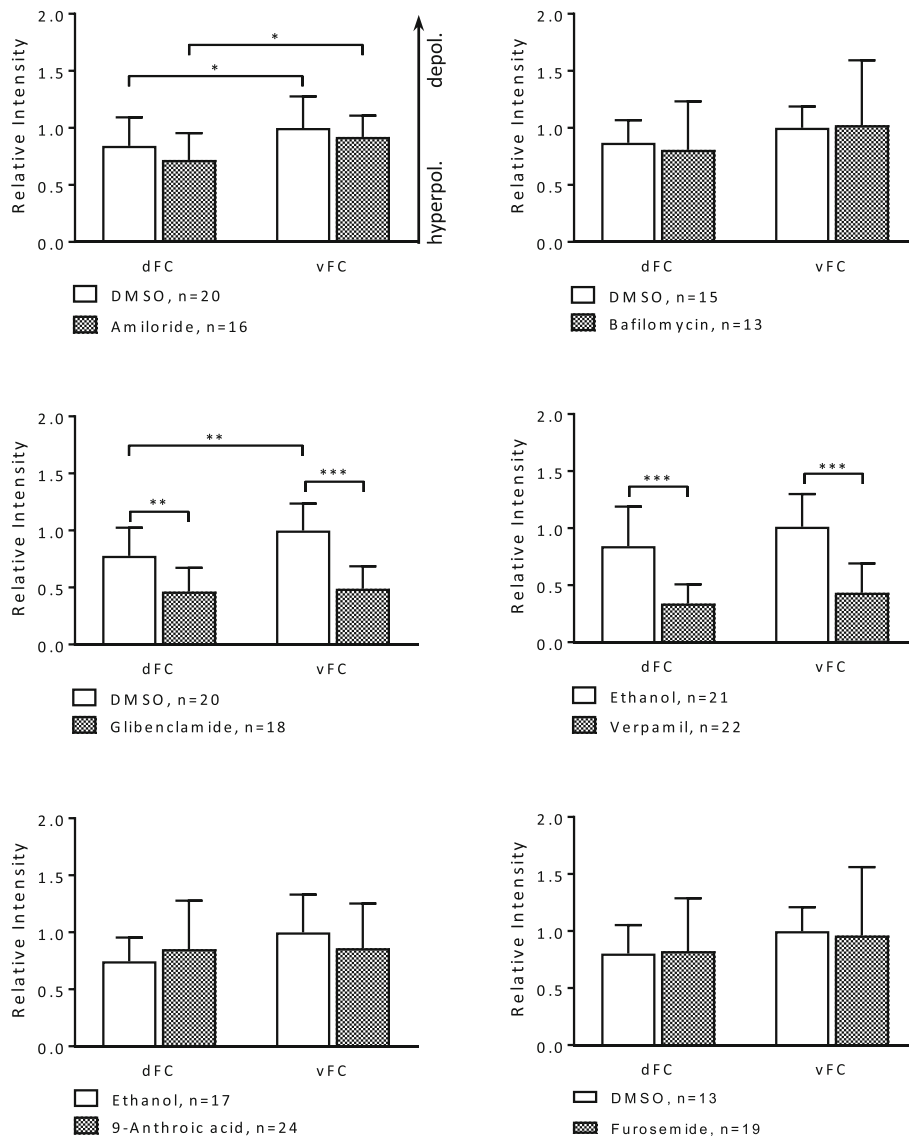
Fig. 8 Some inhibitors exert influence on the d-v V_{mem}-gradient in the FCE during S10b (SIM-experiment; DiBAC). Glibenclamide and verapamil led to hyperpolarisation in both FC types, but especially in vFC, thus lowering the inclination of the d-v gradient (angle $\times 0.1$ and $\times 0.5$, respectively). Amiloride, bafilomycin, 9-anthroic acid and furosemide showed no significant effects on the d-v gradient (cf. Additional file 2: Table S6). For statistics, see legend to Fig. 4

elements is involved in shaping the follicle [42, 43, 62], and stage-specific correlations with pH_i- and V_{mem}-gradients can be observed (unpublished results). Therefore, manipulating the electrochemical gradients and analysing related changes in microfilament and microtubule patterns will help to understand the influence of bioelectrical cues during development (I. Weiß and J. Bohrmann, manuscript in prep.).

Methods
Preparation of *Drosophila* follicles
Oregon R (wild-type) *Drosophila melanogaster* were reared at 20–23 °C on standard medium with additional fresh yeast. 2–3 days old females were killed by crushing the head and thorax with tweezers without anaesthesia. The ovaries were dissected and single follicles of all stages (S1–14) were isolated. The preparations were carried out in R-14 medium [63] which is best suited for in-vitro culture of *Drosophila* follicles [64].
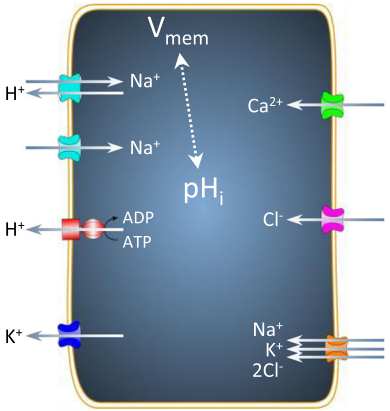
Analysis of intracellular pH
Intracellular pH (pH_i) of FC was analysed using the pH-sensitive fluorescent dye CFDA (5-carboxyfluorescein diacetate, acetoxymethyl ester; 5-CFDA,AM; Molecular Probes/ Thermo Fisher Scientific, USA) [27, 32]. Relative fluorescence intensities were stated, i. e. lower fluorescence intensity

NHEs & Na$^+$-channels (Amiloride)

	WFM	SIM
pH$_i$	No significant effect	Slight acidification
V$_{mem}$	Slight hyper-polarisation	No significant effect

V-ATPases (Bafilomycin)

	WFM	SIM
pH$_i$	No significant effect	Acidification (alkalisation of vesicles)
V$_{mem}$	Slight hyper-polarisation	No significant effect

ATP-sensitive K$^+$-channels (Glibenclamide)

	WFM	SIM
pH$_i$	Strong alkalisation	Strong alkalisation
V$_{mem}$	No significant effect	Hyper-polarisation

L-Type Ca^{2+}-channels (Verapamil)

	WFM	SIM
pH$_i$	Alkalisation	Alkalisation
V$_{mem}$	Strong Hyper-polarisation	Hyper-polarisation

Cl$^-$-channels (9-Anthroic acid)

	WFM	SIM
pH$_i$	Alkalisation	Alkalisation
V$_{mem}$	(Slight) hyper-polarisation	No significant effect

Na$^+$/K$^+$/2Cl$^-$-cotransporters (Furosemide)

	WFM	SIM
pH$_i$	Strong alkalisation	Strong alkalisation
V$_{mem}$	(Slight) hyper-polarisation	No significant effect

pH$_i$

Acidification
+ Amiloride
+ Bafilomycin

Alkalisation
+ Furosemide
+ Glibenclamide
+ 9-Anthroic acid
+ Verapamil

V$_{mem}$

Hyperpolarisation
+ Verapamil
+ Glibenclamide

Slight hyperpolarisation or no clear effect
+ Furosemide
+ 9-Anthroic acid
+ Amiloride
+ Bafilomycin
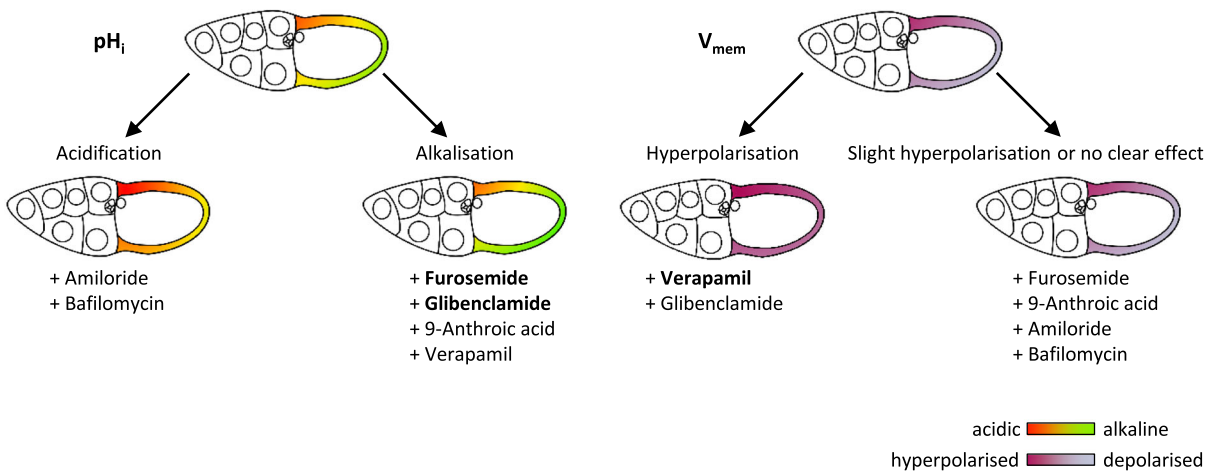
acidic ▮▮▮ alkaline
hyperpolarised ▮▮▮ depolarised

Fig. 9 (See legend on next page.)

> **(See figure on previous page.)**
> **Fig. 9** Summary of the effects of inhibitors on pH_i and V_{mem} in the WFM- and SIM-experiments. Although both experimental conditions led to somewhat different results (upper part), the effects of the inhibitors can be reliably determined (lower part). While inhibition of both $Na^+/K^+/2Cl^-$-cotransporters (furosemide) and ATP-sensitive K^+-channels (glibenclamide) resulted in the most prominent effects on pH_i (strong alkalisation), inhibition of voltage-dependent L-type Ca^{2+}-channels (verapamil) led to the most prominent effect on V_{mem} (strong hyperpolarisation)

indicates lower pH_i (more acidic) while higher fluorescence intensity indicates higher pH_i (more alkaline). Living follicles were incubated for 20 or 60 min, depending on the type of experiment (see below), in R-14 medium containing 4 μM CFDA (dissolved in dimethyl sulfoxide; DMSO). For controls, see Additional file 1: Fig. S3.

Analysis of membrane potential

To analyse membrane potentials (V_{mem}) of FC, the voltage-sensitive fluorescent dye DiBAC (bis-(1,3-dibutylbarbituric acid) trimethine oxonol; $DiBAC_4(3)$; Molecular Probes) was used [28, 32]. Relative fluorescence intensities were stated, i. e. lower fluorescence intensity indicates relative hyperpolarisation and higher fluorescence intensity indicates relative depolarisation. Living follicles were incubated for 20 or 60 min, depending on the type of experiment (see below), in R-14 medium containing 4 μM DiBAC (dissolved in 70% ethanol).

Fluorescence microscopy and optical sectioning

To investigate pH_i and V_{mem} as well as their changes in detail, two types of experiments were performed. ImageJ (NIH, USA) was used to generate pseudocolour images.
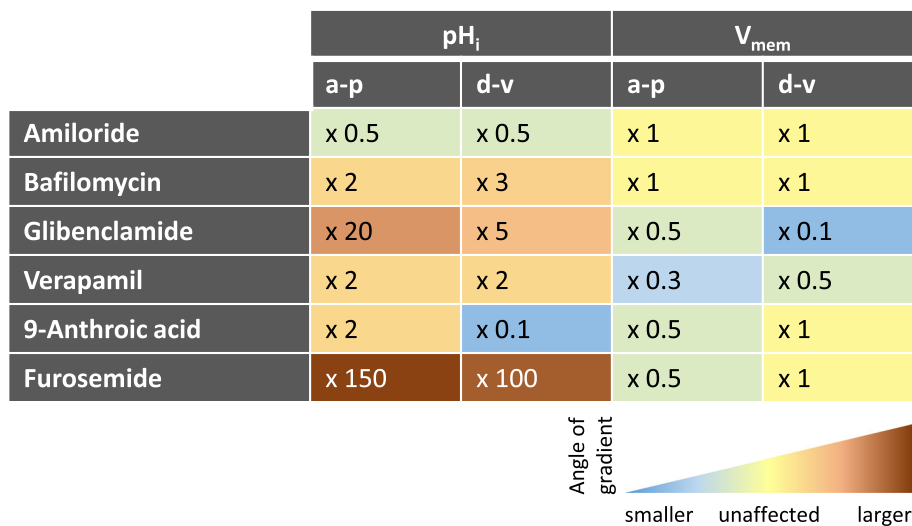
WFM-experiment

Groups of four to ten follicles were imaged for 60 min during staining in covered glass block dishes on a Zeiss Axiovert 200 wide-field fluorescence microscope (WFM), equipped with a Hamamatsu Orca ER camera, using a × 5 objective and a × 1.6 optovar. An image was taken every 5 min. Settings and exposure time remained unchanged.

SIM-experiment

Single follicles were imaged in R-14 medium after staining for 20 min on a Zeiss AxioImager.M2 structured-illumination microscope (SIM), equipped with a Zeiss ApoTome and a Zeiss AxioCamMRm camera, using a × 20 objective. Median optical sections were produced as shown in Fig. 2 a.

Inhibition of ion-transport mechanisms

To compensate for the variability observed between different flies, all S10b-follicles of a single fly (approximately 10–20 follicles) were divided into a control group and an experimental group. Inhibition and staining of living follicles, using either CFDA or

	pH_i		V_{mem}	
	a-p	d-v	a-p	d-v
Amiloride	x 0.5	x 0.5	x 1	x 1
Bafilomycin	x 2	x 3	x 1	x 1
Glibenclamide	x 20	x 5	x 0.5	x 0.1
Verapamil	x 2	x 2	x 0.3	x 0.5
9-Anthroic acid	x 2	x 0.1	x 0.5	x 1
Furosemide	x 150	x 100	x 0.5	x 1

Angle of gradient

smaller   unaffected   larger

Fig. 10 Summary of the influences of inhibitors on the inclinations of the a-p and/or d-v pH_i- and V_{mem}-gradients. Blocking of ion-transport mechanisms resulted in very different effects on the various gradients of relative fluorescence intensity. While, e.g. for the a-p pH_i-gradient, × 0.5 represents a reduction of the angle (decreasing alkalisation, i.e. increasing acidification) by 50% (amiloride; NHEs and Na^+-channels), × 150 means a 150fold enlargement (furosemide; $Na^+/K^+/2Cl^-$-cotransporters) of the angle (increasing alkalisation). The enlargement of the angles caused by bafilomycin (V-ATPases) was due to the alkalisation of vesicles resulting in increased cytoplasmic acidification as well as in shallower pH_i-gradients. E.g., for the d-v V_{mem}-gradient, × 0.1 represents a reduction of the angle (decreasing depolarisation, i.e. increasing hyperpolarisation) by 90% (glibenclamide; ATP-sensitive K^+-channels). The inclinations of the gradients were inferred from the mean values of relative fluorescence intensity shown in Figs. 4b and 5a (pH_i-gradients) and in Figs. 7b and 8 (V_{mem}-gradients), respectively

DiBAC, were done simultaneously for 20 or 60 min, depending on the type of experiment, in R-14 medium containing the respective inhibitor and the fluorescent probe.

The following inhibitors of ion-transport mechanisms were used: Na^+/H^+-exchangers (NHE) and amiloride-sensitive Na^+-channels were blocked with amiloride (Sigma-Aldrich, Germany; 10 μM; dissolved in DMSO), V-ATPases with bafilomycin A1 (Sigma-Aldrich; 160 nM; dissolved in DMSO), ATP-sensitive K^+-channels with glibenclamide (Biomol, Germany; 100 μM; dissolved in DMSO), voltage-dependent L-type Ca^{2+}-channels with verapamil-HCl (Sigma-Aldrich; 50 μM; dissolved in ethanol), Cl^--channels with 9-anthroic acid (Sigma-Aldrich; 100 μM; dissolved in ethanol) and $Na^+/K^+/2Cl^-$-cotransporters with furosemide (Sigma-Aldrich; 1 mM; dissolved in DMSO). Control experiments were performed in R-14 medium containing 0.1–1% v/v ethanol or DMSO, respectively, without the inhibitor.

Quantitative analysis of fluorescence intensities of CFDA and DiBAC

The original grey-scale images were used to measure the fluorescence intensities in the FCE with ImageJ ("mean grey value").

WFM-experiment

WFM-images of each point of time were evaluated by measuring the columnar FCE of every single follicle. The mean grey values of the experimental group and the control group, respectively, were averaged (all follicles from the same fly). To compare the long-term effects of the inhibitors on either pH_i or V_{mem}, the averaged values of each point of time were summed up and normalised. Three experiments for each inhibitor were included in this evaluation (*mean intensity ratio*).

SIM-experiment

SIM-images were used to measure individual regions of different types of FC: cFC, mbFC, pFC, dFC and vFC (see Fig. 1 a). All mean grey values of each FC type of the experimental group and the control group, respectively, were averaged for comparative analysis (all follicles from the same fly). For each inhibitor, at least five repetitions of the experiment were performed. The normalised values of the single experiments were merged into one evaluation (*relative intensity*).

Multiple t-tests with Holm-Sidak correction, Microsoft Excel and GraphPad Prism were used for statistical analysis. Graphpad Prism was also used for representation of the data.

Additional files

Additional file 1: Figure S1. Development of pH_i-gradients in the FCE during S8–12 (CFDA; SIM). Examples corresponding to Fig. 1b. **Figure S2.** Development of V_{mem}-gradients in the FCE during S8–12 (DiBAC; SIM). Examples corresponding to Fig. 2b. **Figure S3.** Controls for pH_i (CFDA; WFM). Examples of S10b follicles incubated for 60 min in R-14 medium pH 5.5 (hydrochloric acid) and pH 8.0 (sodium hydroxide), respectively. (PPTX 9873 kb)

Additional file 2: Table S1. Development of pH_i-gradients in the FCE during S8–12 (CFDA; SIM). Numerical values corresponding to Fig. 1 c. **Table S2.** Development of V_{mem}-gradients in the FCE during S8–12 (DiBAC; SIM). Numerical values corresponding to Fig. 2 c. **Table S3.** Inhibitors of ion-transport mechanisms exert influence on the pH_i in the FCE during S10b (WFM-experiment; CFDA). Numerical values corresponding to Fig. 3a. **Table S4.** Inhibitors of ion-transport mechanisms exert influence on the V_{mem} in the FCE during S10b (WFM-experiment; DiBAC). Numerical values corresponding to Fig. 6a. **Table S5.** The a-p and d-v pH_i-gradients in the FCE are affected by all inhibitors in S10b (SIM-experiment; CFDA). Numerical values corresponding to Figs. 4b and 5a. **Table S6.** The a-p V_{mem}-gradient in the FCE is affected by most inhibitors in S10b. Some inhibitors exert influence on the d-v V_{mem}-gradient (SIM-experiment; DiBAC). Numerical values corresponding to Figs. 7b and 8. (PPTX 78 kb)

Abbreviations

aFC: anterior follicle cells; a-p: antero-posterior; cFC: centripetal follicle cells; CFDA : 5-carboxyfluorescein diacetate, acetoxymethyl ester; DiBAC: bis-(1,3-dibutylbarbituric acid) trimethine oxonol; DIC: differential-interference contrast; DMSO: dimethyl sulfoxide; d-v: dorso-ventral; FC: follicle cells; FCE: follicle-cell epithelium; mbFC: mainbody follicle cells; NC: nurse cells; NHE: Na^+/H^+-exchangers; Oo: oocyte; pFC: posterior follicle cells; pH_i: intracellular pH; S: stage; SIM: structured-illumination microscopy; V_{mem}: membrane potential; WFM: wide-field microscopy

Availability of data and materials
The datasets used during the current study are available from the corresponding author on reasonable request.

Ethics approval and consent to participate
Not applicable.

Consent for publication
Not applicable.

Competing interests
The authors declare that they have no competing interests.

References
1. McLaughlin KA, Levin M. Bioelectric signaling in regeneration: mechanisms of ionic controls of growth and form. Dev Biol. 2018;433:177–89.
2. Pietak A, Levin M. Bioelectrical control of positional information in development and regeneration: a review of conceptual and computational advances. Prog Biophys Mol Bio. 2018;137:52–68.
3. Cervera J, Manzanares JA, Mafe S. Cell-cell bioelectrical interactions and local heterogeneities in genetic networks: a model for the stabilization of

single-cell states and multicellular oscillations. Phys Chem Chem Phys. 2018; 20:9343–54.

4.   McCaig CD, Rajnicek AM, Song B, Zhao M. Controlling cell behavior electrically: current views and future potential. Physiol Rev. 2005;85:943–78.

5.   Chang F, Minc N. Electrochemical control of cell and tissue polarity. Annu Rev Cell Dev Biol. 2014;30:317–36.

6.   Stock C, Ludwig FT, Hanley PJ, Schwab A. Roles of ion transport in control of cell motility. Compr Physiol. 2013;3:59–119.

7.   Blackiston DJ, McLaughlin KA, Levin M. Bioelectric controls of cell proliferation: ion channels, membrane voltage and the cell cycle. Cell Cycle. 2009;8:3527–36.

8.   Ulmschneider B, Grillo-Hill BK, Benitez M, Azimova DR, Barber DL, Nystul TG. Increased intracellular pH is necessary for adult epithelial and embryonic stem cell differentiation. J Cell Biol. 2016;215:345–55.

9.   Amith SR, Wilkinson JM, Fliegel L. Na$^+$/H$^+$ exchanger NHE1 regulation modulates metastatic potential and epithelial-mesenchymal transition of triple-negative breast cancer cells. Oncotarget. 2016;7:21091–113.

10. Tatapudy S, Aloisio F, Barber D, Nystul T. Cell fate decisions: emerging roles for metabolic signals and cell morphology. EMBO Rep. 2017;18: 2105–18.

11. Putney LK, Barber DL. Na-H exchange-dependent increase in intracellular pH times G2/M entry and transition. J Biol Chem. 2003;278:44645–9.

12. Musgrove E, Seaman M, Hedley D. Relationship between cytoplasmic pH and proliferation during exponential growth and cellular quiescence. Exp Cell Res. 1987;172:65–75.

13. Aw S, Koster JC, Pearson W, Nichols CG, Shi N-Q, Carneiro K, Levin M. The ATP-sensitive K$^+$-channel (K$_{ATP}$) controls early left-right patterning in *Xenopus* and chick embryos. Dev Biol. 2010;346:39–53.

14. Beane WS, Morokuma J, Adams DS, Levin M. A chemical genetics approach reveals H,K-ATPase-mediated membrane voltage is required for planarian head regeneration. Chem Biol. 2011;18:77–89.

15. Inaba M, Yamanaka H, Kondo S. Pigment pattern formation by contact-dependent depolarization. Science. 2012;335:677.

16. Simons M, Gault WJ, Gotthardt D, Rohatgi R, Klein TJ, Shao Y, Lee H-J, Wu A-L, Fang Y, Satlin LM, Dow JT, Chen J, Zheng J, Boutros M, Mlodzik M. Electrochemical cues regulate assembly of the frizzled/Dishevelled complex at the plasma membrane during planar epithelial polarization. Nat Cell Biol. 2009;11:286–94.

17. Webb BA, Chimenti M, Jacobson MP, Barber DL. Dysregulated pH: a perfect storm for cancer progression. Nat Rev Cancer. 2011;11:671–7.

18. White KA, Grillo-Hill BK, Barber DL. Cancer cell behaviors mediated by dysregulated pH dynamics at a glance. J Cell Sci. 2017;130:663–9.

19. Yang M, Brackenbury WJ. Membrane potential and cancer progression. Front Physiol. 2013;4:185.

20. Harguindey S, Reshkin SJ, Orive G, Arranz JL, Anitua E. Growth and trophic factors, pH and the Na$^+$/H$^+$ exchanger in Alzheimer's disease, other neurodegenerative diseases and cancer: new therapeutic possibilities and potential dangers. Curr Alzheimer Res. 2007;4:53–65.

21. Levin M, Pezzulo G, Finkelstein JM. Endogenous bioelectric signaling networks: exploiting voltage gradients for control of growth and form. Annu Rev Biomed Eng. 2017;19:353–87.

22. Levin M. Endogenous bioelectrical networks store non-genetic patterning information during development and regeneration. J Physiol. 2014;592: 2295–305.

23. Adams DS, Levin M. Endogenous voltage gradients as mediators of cell-cell communication: strategies for investigating bioelectrical signals during pattern formation. Cell Tissue Res. 2013;352:95–122.

24. FitzHarris G, Baltz JM. Granulosa cells regulate intracellular pH of the murine growing oocyte via gap junctions: development of independent homeostasis during oocyte growth. Development. 2006;133:591–9.

25. Mathews J, Levin M. Gap junctional signaling in pattern regulation: physiological network connectivity instructs growth and form. Dev Neurobiol. 2017;77:643–73.

26. Cervera J, Pietak A, Levin M, Mafe S. Bioelectrical coupling in multicellular domains regulated by gap junctions: a conceptual approach. Bioelectrochemistry. 2018;123:45–61.

27. Han J, Burgess K. Fluorescent indicators for intracellular pH. Chem Rev. 2010; 110:2709–28.

28. Adams DS, Levin M. Measuring resting membrane potential using the fluorescent voltage reporters DiBAC$_4$(3) and CC2-DMPE. Cold Spring Harb Protoc. 2012;(4):459–64.

29. Overall R, Jaffe LF. Patterns of ionic current through *Drosophila* follicles and eggs. Dev Biol. 1985;108:102–19.

30. Bohrmann J, Dorn A, Sander K, Gutzeit H. The extracellular electrical current pattern and its variability in vitellogenic *Drosophila* follicles. J Cell Sci. 1986; 81:189–206.

31. Bohrmann J, Huebner E, Sander K, Gutzeit H. Intracellular electrical potential measurements in *Drosophila* follicles. J Cell Sci. 1986;81: 207–21.

32. Krüger J, Bohrmann J. Bioelectric patterning during oogenesis: stage-specific distribution of membrane potentials, intracellular pH and ion-transport mechanisms in *Drosophila* ovarian follicles. BMC Dev Biol. 2015;15:1.

33. Lautemann J, Bohrmann J. Relating proton pumps with gap junctions: colocalization of ductin, the channel-forming subunit c of V-ATPase, with subunit a and with innexins 2 and 3 during *Drosophila* oogenesis. BMC Dev Biol. 2016;16:24.

34. Sun YA, Wyman RJ. Reevaluation of electrophoresis in the *Drosophila* egg chamber. Dev Biol. 1993;155:206–15.

35. Munley SM, Kinzeler S, Lizzano R, Woodruff Rl. Fractional contribution of major ions to the membrane potential of *Drosophila melanogaster* oocytes. Arch Insect Biochem. 2009;70:230–43.

36. Bohrmann J. Potassium uptake into *Drosophila* ovarian follicles: relevance to physiological and developmental processes. J Insect Physiol. 1991;37:937–46.

37. Mahowald AP, Kambysellis MP. Oogenesis. In: Ashburner M, Wright TRF, editors. Genetics and biology of *Drosophila*. New York: Academic Press; 1980. p. 141–224.

38. González-Reyes A, St Johnston D. Patterning of the follicle cell epithelium along the anterior-posterior axis during *Drosophila* oogenesis. Development. 1998;125:2837–46.

39. Wu X, Tanwar PS, Raftery LA. *Drosophila* follicle cells: morphogenesis in an eggshell. Semin Cell Dev Biol. 2008;19:271–82.

40. Cavaliere V, Bernardi F, Romani P, Duchi S, Gargiulo G. Building up the *Drosophila* eggshell: first of all the eggshell genes must be transcribed. Dev Dyn. 2008;237:2061–72.

41. Riechmann V, Ephrussi A. Axis formation during *Drosophila* oogenesis. Curr Opin Genet Dev. 2001;11:374–83.

42. Gates J. *Drosophila* egg chamber elongation: insights into how tissues and organs are shaped. Fly. 2012;6:213–27.

43. Viktorinová I, Henry I, Tomancak P. Epithelial rotation is preceded by planar symmetry breaking of actomyosin and protects epithelial tissue from cell deformations. PLoS Genetic. 2017;13:e1007107.

44. Bohrmann J, Braun B. Na,K-ATPase and V-ATPase in ovarian follicles of *Drosophila melanogaster*. Biol Cell. 1999;91:85–98.

45. Bohrmann J, Zimmermann J. Gap junctions in the ovary of *Drosophila melanogaster*: localization of innexins 1, 2, 3 and 4 and evidence for intercellular communication via innexin-2 containing channels. BMC Dev Biol. 2008;8:111.

46. Bohrmann J, Haas-Assenbaum A. Gap junctions in ovarian follicles of *Drosophila melanogaster*: inhibition and promotion of dye-coupling between oocyte and follicle cells. Cell Tissue Res. 1993;273:163–73.

47. Giannakou ME, Dow JA. Characterization of the *Drosophila melanogaster* alkali-metal/proton exchanger (NHE) gene family. J Exp Biol. 2001;204: 3703–16.

48. Bohrmann J, Heinrich UR. Localisation of potassium pumps in *Drosophila* ovarian follicles. Zygote. 1994;2:189–99.

49. Darboux I, Lingueglia E, Champigny G, Coscoy S, Barbry P, Lazdunski M. dGNaC1, a gonad-specific amiloride-sensitive Na$^+$ channel. J Biol Chem. 1998;273:9424–9.

50. Robinson SW, Herzyk P, Dow JAT, Leader DP. FlyAtlas: database of gene expression in the tissues of *Drosophila melanogaster*. Nucleic Acids Res. 2013;41:D744–50.

51. Wieczorek H, Putzenlechner M, Zeiske W, Klein U. A vacuolar-type proton pump energizes K$^+$/H$^+$ antiport in an animal plasma membrane. J Biol Chem. 1991;266:15340–7.

52. Adler S, Fraley DS. Potassium and intracellular pH. Kidney Int. 1977;11: 433–42.

53. Sherwood AC, John-Alder K, Sanders MM. Characterization of chloride uptake in *Drosophila* kc cells. J Cell Physiol. 1988;136:500–6.

54. Ianowski JP, O'Donnell MJ. Basolateral ion transport mechanisms during fluid secretion by *Drosophila* Malpighian tubules: Na$^+$ recycling, Na$^+$:K$^+$:2Cl$^-$ cotransport and Cl$^-$ conductance. J Exp Biol. 2004;207:2599–609.

55. Hoffmann EK. Anion exchange and anion-cation co-transport systems in mammalian cells. Philos Trans Royal Soc. 1982;299:519–35.
56. Benitez M, Tatapudy S, Liu Y, Barber DL, Nystul TG. *Drosophila anion exchanger 2* is required for proper ovary development and oogenesis. Dev Biol. 2019. https://doi.org/10.1016/j.ydbio.2019.04.018.
57. Putney LK, Denker SP, Barber DL. The changing face of the Na^+/H^+ exchanger, NHE1: structure, regulation, and cellular actions. Annu Rev Pharmacol Toxicol. 2002;42:527–52.
58. Donowitz M, Li X. Regulatory binding partners and complexes of NHE3. Physiol Rev. 2007;87:825–72.
59. Wang Y, Telfer WH. Cyclic-AMP-induced water uptake in a moth ovary: inhibition by bafilomycin and anthracene-9-carboxylic acid. J Exp Biol. 1998; 201:1627–35.
60. Harvey WR, Wieczorek H. Animal plasma membrane energization by chemiosmotic H^+ V-ATPases. J Exp Biol. 1997;200:203–16.
61. Clapham DE. Calcium signaling. Cell. 2007;131:1047–58.
62. Gutzeit HO. Organization and in vitro activity of microfilament bundles associated with the basement membrane of *Drosophila* follicles. Acta Histochem. 1992; Suppl. XLI:201–10.
63. Robb JA. Maintenance of imaginal discs of *Drosophila melanogaster* in chemically defined media. J Cell Biol. 1969;41:876–85.
64. Bohrmann J. In vitro culture of *Drosophila* ovarian follicles: the influence of different media on development, RNA synthesis, protein synthesis and potassium uptake. Roux Arch Dev Biol. 1991;199:315–26.

Publisher's Note

Springer Nature remains neutral with regard to jurisdictional claims in published maps and institutional affiliations.